Antiproliferative Activity, Preliminary QSAR Analysis and in silico ADME Studies of Morita-Baylis-Hillman Adducts from Isatin Derivatives in Four Cancer Cell Lines

Atividade antiproliferativa, análise QSAR preliminar e estudos in silico ADME de adutos de Morita-Baylis-Hillman de derivados de isatina em quatro linhagens de células de câncer

Gilmar F. dos Santos,[a] Gardenia C. G. Militão,[b] Thiago D. S. Silva,[a] Júlia L. C. de Souza, Vinícius B. M. de Brito,[a] Eduardo D. S. Mourão,[b] Mário L. A. A. Vasconcellos, Edilson B. Alencar-Filho,[c] Claudio Gabriel Lima-Junior[a],*

a Federal University of Paraíba, Department of Chemistry, Campus I, CEP 8051-900, João Pessoa-PB, Brazil.
b Federal University of Pernambuco, Department of Physiology and Pharmacology, CEP 50670-901, Recife-PE, Brazil.
c Federal University of San Francisco Valley, Collegiate of Pharmaceutical Sciences, CEP 56304-205, Petrolina-PE, Brazil.

*E-mail: claudio@quimica.ufpb.br

We present here the antitumor activity of 21 Morita-Baylis-Hillman adducts (MBHA), synthesized by us, followed by structural insights obtained from QSAR and ADME *in silico* analyses. The activities were determined in four different cancer cell lines, including HL60 (human promyelocytic leukemia), MCF-7 (human breast adenocarcinoma), Hep-2 (cervix carcinoma) and HepG2 (hepatocellular carcinoma). Some of compounds had higher selectivity index (SI) than Doxorubicin. For example, 6 and 9 presented IC_{50} of 48 nM and 42 nM against human promyelocytic leukemia, with an SI of 282.10 and 170.00, respectively. Doxorubicin presented $IC_{50} = 110$ nM, with only 12.73 of SI. QSAR procedures provided interesting mathematical models, showing the importance of the nitrile and allyl moieties as well as the possibility of changes in the six-membered ring or isatin nitrogen substituents. SwissADME *in silico* analysis revealed important discussions about structural requirements for a better pharmacokinetic profile, in future lead optimizations.

Keywords Morita-Baylis-Hilman adducts from isatin derivatives; antiproliferative activity; Selectivity Index; QSAR; *in silico* ADME.

1. Introduction

Cancer is one of the most important diseases, being responsible for a large number of deaths around the world. The International Agency for Research on Cancer estimates the incidence of mortality and prevalence from major types of cancer for 185 countries, revealing that there were 18.1 million new cancer cases and 9.6 million of cancer deaths in 2018.[1]

Among others strategies, the chemotherapy is an important tool used for cancer treatments. However, the side-effects and long-term sequel of anti-cancer compounds remain a major source of inconvenience for both patients and clinicians, despite of the improved efficacy and survival offered by modern treatments.[2] Current drugs or other approaches to counteract chemotherapy-induced adverse effects are often incompletely effective. Thus, there is a constant search for new compounds with anticancer property, with minimal side effects.[2]

Focusing on the molecular perspective, the 3-Hydroxyl-3-substituted oxindole core has been receiving prominence in the scientific community, due its presence in natural products with antiproliferactive activity, for example, in the scaffold of the alkaloid convolutamydine A.[3] On the other hand, the same oxindole core can be accessed synthetically by the Morita-Baylis-Hillman Reaction (MBHR) between an isatin nucleus (Figure 1) and a Michael acceptor, catalyzed by 1,4-diazabicyclo[2.2.2]octane (DABCO).[4,5] In this context, recently we reported the good antiproliferative activity of some MBHA in one specific cancer cell line (lung cancer),[6] encouraging the investigation of more cell types in the continuous effort of our research group.

Considering the Medicinal Chemistry approaches in the investigation of potential drugs, *in silico* models have been emerged as useful strategies to obtain rationalized information about the structure-activity relationships.[7] In this way, the Quantitative Structure-Activity Relationship (QSAR) have been used to detect some molecular characteristics that have more influence in biological responses, providing mathematical models to predict activities of analog compounds.[8,9] In addition, *in silico* predictions about ADME (Absorption, Distribution,
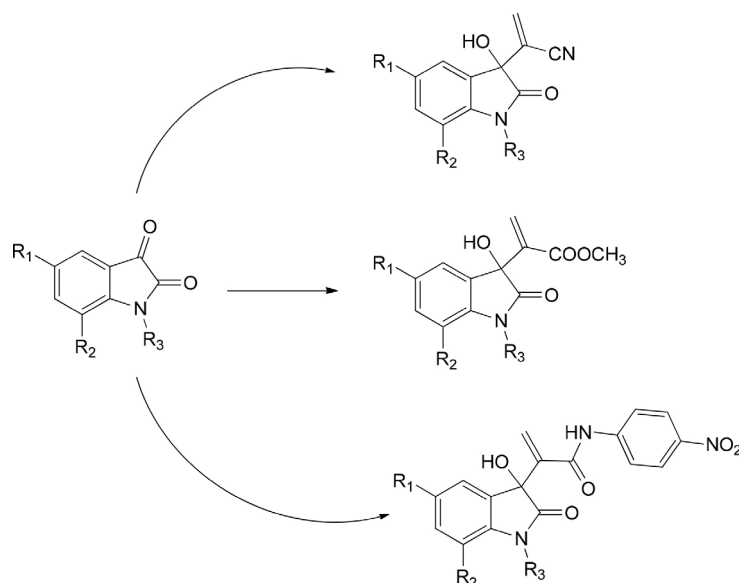
Figure 1. Hydroxy-3-substituted oxindole core obtained by MBHR[6]

Metabolism, Excretion) profile can provide possible pharmacokinetic behaviors, being a useful tool in lead optimizations by the modern pharmaceutical companies.

In this paper, we present the antiproliferative activity of 21 MBHA from isatin derivatives, synthetized by our Laboratory, in four cancer cell lines, followed by QSAR modellings and *in silico* analysis of their ADME profile.

2. Material and Methods

2.1. Chemistry

Morita-Baylis-Hillman adducts **1–21** (Figure 2) were synthesized according to our previously reported procedures.[6] The molecular diversity was obtained by different strategies.[6] Initially, the commercially available isatin was N-alkylated using allyl bromide or methyl iodide. To prepare the 5-nitroisatin, a mixture of $NaNO_3$ and H_2SO_4 was used. The aromatic chlorination of the isatin was

performed with trichloroisocyanuric acid (TCCA) using sulfuric acid as a catalyst.

2.2. *In vitro* antiproliferative activity

Human tumor cell lines HL-60 (promyelocytic leukemia), MCF-7 (breast adenocarcinoma), HepG2 (hepatocellular carcinoma) and Hep-2 (cervix carcinoma) were obtained from Rio de Janeiro Cell Bank (Rio de Janeiro, Brazil). In addition, were also used human peripheral blood mononuclear cells (PBMCs), obtained from healthy volunteers. The PBMCs were isolated according to the standard method of density-gradient centrifugation over Ficoll-Histopaque. The protocol (CAAE: 66925717.2.0000.5208) was approved by the Ethics Committee of the Federal University of Pernambuco. The cells were maintained in RPMI 1640 medium or DMEN supplemented with 10% fetal bovine serum, 2 mM glutamine, 100 U/mL penicillin, 100 µg/mL streptomycin (Gigco™ Life Technologies, USA) at 37°C with 5%

(1) $R_1 = R_2 = R_3 = H$
(2) $R_1 = R_2 = H$; $R_3 = CH_3$
(3) $R_1 = R_2 = H$; $R_3 = allyl$
(4) $R_1 = NO_2$; $R_2 = R_3 = H$
(5) $R_1 = NO_2$; $R_2 = H$; $R_3 = CH_3$
(6) $R_1 = NO_2$; $R_2 = H$; $R_3 = allyl$
(7) $R_1 = R_2 = Cl$; $R_3 = H$
(8) $R_1 = R_2 = Cl$; $R_3 = CH_3$
(9) $R_1 = R_2 = Cl$; $R_3 = allyl$

(10) $R_1 = R_2 = R_3 = H$
(11) $R_1 = R_2 = H$; $R_3 = CH_3$
(12) $R_1 = R_2 = H$; $R_3 = allyl$
(13) $R_1 = NO_2$; $R_2 = R_3 = H$
(14) $R_1 = NO_2$; $R_2 = H$; $R_3 = CH_3$
(15) $R_1 = NO_2$; $R_2 = H$; $R_3 = allyl$
(16) $R_1 = R_2 = Cl$; $R_3 = H$
(17) $R_1 = R_2 = Cl$; $R_3 = CH_3$

(18) $R_1 = R_2 = H$; $R_3 = CH_3$
(19) $R_1 = R_2 = H$; $R_3 = allyl$
(20) $R_1 = R_2 = Cl$; $R_3 = CH_3$
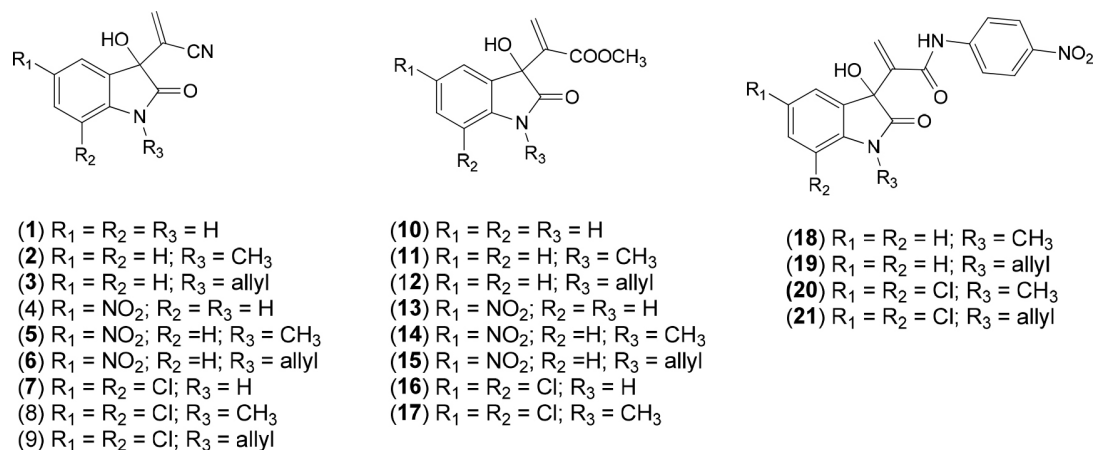**(21)** $R_1 = R_2 = Cl$; $R_3 = allyl$

Figure 2. MBHA from isatin derivatives studied in this work

CO_2. To assess the cytotoxicity of the compounds, the 3-(4,5-dimethyl-2-thiazolyl)-2,5-diphenyl-2H tetrazolium bromide (MTT, Sigma-Aldrich-USA) reduction assay was used after 72 h incubation. For all experiments, cells were plated in 96-well plates (105 cells/mL for adherent cells or 3 x 105 cells/mL for the leukemia and 106 for PBMC). After 24 h, the compounds, diluted in complete medium with 0.5 % dimethylsulfoxide (DMSO, Vetec, Brazil), in concentrations ranging from 0.03 to 25 µg/mL were added to each well. Negative control received the same amount of DMSO. Doxorubicin (Sigma-Aldrich, USA) (0.01-5 µg/mL) was used as the positive control. After 69 h of treatment, 20 µL of MTT (5 mg/mL, Sigma Aldrich Co., St. Louis, MO, USA) was added. In the end of the incubation, the MTT formazan product was dissolved in 100 µL of DMSO and the absorbance was measured at 595 nm in a plate spectrophotometer (Varioskan Flash; Thermo Scientific, Finland).

2.3. QSAR and ADME *in silico* procedures

Molecular structures of isatin derivatives were submitted to initial geometry optimization using PM6 semi-empirical Hamiltonian,[10] followed by a relaxed scan in the molecular degrees of freedom (dihedral angles). The most stable minimum for each compound was submitted finally to DFT calculations using the hybrid functional B3LYP/6-311++(d,p).[11-13] The vibrational frequencies were obtained to check the minimal geometries. All these calculations were made using Gaussian09W,[14] program at CENAPAD-UFC cluster environment.

The optimized geometries were submitted to E-Dragon online platform,[15] in order to the calculations of molecular descriptors. An initial matrix with 1666 independent variables was submitted to a variable selection procedure using the Ordered Predictors Selector (OPS) algorithm,[16] implemented on QSAR modelling software.[17]

The biological activities (Y) were converted to the $Log(1/IC_{50})$ (pIC_{50}), considering each cytotoxic activity against MCF-7, HEP4 and HL-60 (HepG2 was not used due the few values available). Compounds with undefined IC_{50} were not used (values expressed as >50). Then, three models were investigated. The number and type of the compounds used were different for each activity, considering the available data (Table 5). After OPS procedures, a set of several descriptors were obtained for each activity. Training and test sets were defined, the last considering around 20% of the total number of compounds, randomly selected in view of structural and activity variability. An additional systematic search (MLR based) was conducted on the three data sets, using the BuildQSAR software reducing the final number of descriptors.[18] Validation parameters of QSAR modelling were based on the coefficient of determination for calibration (R^2); adjusted coefficient of determination for calibration (R^2_{adj}); coefficient of determination for leave-one-out cross-validation (Q^2); coefficient of determination for external validation (Q^2_{ext}); F-test value (F); standard deviation of estimated Y (s); evaluation of the correlation between descriptors and Pearson's correlation coefficient of the models (R_{cal}).[19]

The evaluation of the ADME profile was made for the compounds with calculated Selectivity Index, using the SwissADME platform.[20] This approach gives to us an idea about the pharmacokinetic behaviour of the highlighted molecules, contributing in the rational projection of lead compounds.

3. Results and Discussion

3.1. *In vitro* proliferative activity of the 21 synthetic MBHA

The antiproliferative activity of MBHA from isatin derivatives was obtained for four different cell lines, including HL60 (human promyelocytic leukemia), MCF-7 (human breast adenocarcinoma), Hep-2 (cervix carcinoma) and HepG2 (hepatocellular carcinoma). The MTT colorimetric assay was employed to obtain the potency of the compounds. The results are summarized in Table 1, where Doxorubicin was used as a positive control.

It can be observed that the MBHA presenting nitrile group are more active than carboxymethylester analogs (Table 1), except by **4**. This experimental result is quite interesting, considering the increase in the number of drugs containing the nitrile group as part of their pharmacophoric group.[21]

Compounds with $IC_{50} \leq 3$ µM can be judged as highly actives; values in the range of 3–6 µM show good activity. On the other hand, compounds with IC_{50} between 6 µM and 12 µM can be considered with moderate activity, and values in the range of 12 – 24 µM can be considered as having low activity.[22] In this way, we can observe that the HL60 cell line was the most sensitive one, since most of the tested adducts exhibited good to high levels of potency (Table 1). Only five MBHA presented moderate activity against HL60 cell line. The HepG2 cell line was the less sensitive. Only **7** was potent against HepG2 and other MBHA displayed low activity (**5** and **8**). We can also observe that the compounds **18**-**21** were essentially inactive in most of the cell lines, presenting good activity only against HL60.

In order to demonstrate if the cytotoxic effect presented by MBHA was selective to cancer cells, compounds **2**-**3** and **5**-**9** were screened against normal Human Peripheral Blood Mononuclear Cells (PBMCs) and the results are in the Table 2.

The major obstacle in the cancer chemoterapy is the selectivity of the drug to eliminate the harmful cells without damaging the healthy cells, avoiding side effects. In this way, the selectivity index (SI) of a new chemotherapeutic agent is a good indicative of the potential safety. The Table 2 shows that, with the exception of MCF-7, some compounds

Table 1. Cytotoxic activity of the MBHA against four different cancer cell lines*

MBHA	MCF-7	HEP-2	HL60	HepG2
1	6.0 (5.0–7.0)	3.4 (2.85–4.00)	3.60 (2.65–3.05)	17.45 (13.70–22.19)
2	11.59 (7.36– 18.86)	4.06 (3.27–5.05)	1.77 (3.70–5.19)	29.25 (22.99–37.29)
3	4.20 (3.92–4.50)	2.33 (1.96–2.79)	1.83 (1.59–2.13)	19.58 (14.60–25.88)
4	>50	>50	>50	>50
5	6.49 (5.95– 7.03)	5.79 (5.02–6.56)	2.93 (2.70 –3.17)	11.78 (9.34–14.83)
6	6.88 (5.93 –8.04)	5.96 (4.91–7.37)	0.048 (0.035–0.063)	8.04 (6.28– 10.32)
7	8.39 (6.82– 9.10)	5.22 (4.10 – 6.72)	1.30 (1.16– 1.45)	2.54 (2.09– 3.06)
8	9.57 (8.65 –10.60)	2.10 (1.81–2.41)	1.42 (1.28–1.52)	12.34 (10.43–14.18)
9	3.90 (3.27 –4.84)	3.90 (3.25–4.55)	0.042 (0.035–0.052)	9.81 (8.34–11.56)
10	>50	48.80 (40.30– 59.06)	27.51 (21.67–34.98)	>50
11	25.18 (21.21–29.92)	38.22 (29.15 –50.17)	17.25 (11.54 –25.83)	>50
12	18.02 (12.60–25.82)	32.42 (26.04– 40.40)	16.08 (12.93 –20.00)	>50
13	>50	>50	>50	>50
14	34.25 (31.93–46.60)	21.37 (18.30 –31.70)	6.27 (5.48– 9.11)	48.70 (44.28–66.49)
15	7.55 (5.50– 10.30)	30.72 (24.94–37.83)	5.42 (4.34 –6.76)	40.89 (33.84–49.43)
16	7.52 (5.35–10.60)	6.68 (5.55–8.04)	4.76 (3.92– 5.75)	34.75 (27.14–44.45)
17	30.32 (25.97– 35.43)	>50	4.20 (3.40 –5.14)	31.08 (26.57–36.41)
18	66.40 (43.80– 100.68)	18.79 (12.49 –29.24)	18.04 (12.66 –27.72)	NT
19	38.88 (30.80 –49.05)	>50	5.49 (3.73– 8.03)	NT
20	41.98 (36.41– 48.36)	18.73 (11.87– 26.60)	5.38 (3.43 –8.42)	NT
21	>50	42.19 (23.85 –74.68)	14.14 (8.90 –22.50)	NT
Doxoru-bicin	0.37 (0.18–0.92)	1.3 (0.55–2.6)	0.11 (0.1–0.33)	0.6 (0.51–0.81)

*The data are presented as IC_{50} values in µM, obtained by non-linear regression. NT = Not tested

Table 2. Cytotoxic activity of **2-3** and **5-9** against Human Peripheral Blood Mononuclear Cells (PBMC)*

Entry	Compound	$IC_{50 µM\ PBMC}$ [a]	SI_{MCF-7}	SI_{HEP-2}	SI_{HL60}	SI_{HepG2}
1	**2**	14.72 (11.03-19.63)	1.27	**3.63**	8.32	0.50
2	**3**	2.75 (1.96-3.83)	0.65	1.18	1.50	0.14
3	**5**	11.16 (8.57-14.48)	1.72	1.93	3.81	0.95
4	**6**	13.54 (11.23-16.35)	1.97	2.27	**282.1**	1.68
5	**7**	6.79 (5.19-8.89)	0.81	1.30	5.22	**2.67**
6	**8**	8.40 (6.10-11.67)	0.88	4.0	5.91	0.68
7	**9**	7.14 (5.68-8.96)	1.83	1.83	**170**	0.73
8	Doxorubicin	1.4 (0.9-2.6)	**3.78**	1.08	12.73	2.33

*Data are presented as IC_{50} values (µM) obtained by non-linear regression. SI (selectivity index of specific cell line) = IC_{50} PBMC/IC_{50} cell line

synthetized by our group presented higher selectivity index than Doxorubicin (standard drug). The compound **2** (Entry 1) is the most selective to HEP-2 cancer cell line, **7** to HepG2 (Entry 5) and **6** and **9** to HL60, showing the highest selectivity index (SI > 100) (Entry 4, SI = 282.1 and entry 7, SI = 170). These results put these compounds as promising anticancer agents, displaying yet suitable potency against at least two of the four cancer cell lines.

3.2. *In silico* modelling

After the experimental work, three QSAR models were developed for the available data and the results are presented below (HepG2 was not considered due the absence of IC_{50} for nine compounds). The chiral profile of the compounds discourages the use of 3D or multiD-QSAR models, considering that the biological tests were made with racemic mixture. Thus, the use of classical or constitutional/topologic descriptors was most convenient, since their values are the same for different enantiomers. The Table 3 shows the values of the selected descriptors for each activity, denoting the molecular features most important to explain the biological variability, expressed by **pIC_{50}**.

The equations of the QSAR models are presented below. The analysis of the correlation between the independent variables showed that all values were less than 0.6.

Table 3. pIC_{50} values for the cancer cell lines and E-Dragon molecular descriptors selected by OPS/Systematic search algorithms

MCF-7				
MBHA	**pIC_{50}**	**L2p**	**RDF085u**	**N-R**
1	5.22	1.654	0.002	0
2	4.93	2.729	0.002	1
3	5.37	3.698	1.276	1
5*	5.18	3.176	0.011	1
6	5.16	4.405	0.932	1
7	5.07	2.266	0.145	0
8	5.01	3.314	0.811	1
9	5.4	4.478	1.383	1
11*	4.59	2.453	4.904	1
12	4.74	4.308	9.486	1
14	4.46	2.891	4.293	1
15	5.12	5.092	8.114	1
16*	5.12	2.037	3.133	0
17	4.51	2.975	3.755	1
18	4.17	2.205	9.15	1
19	4.41	2.712	9.519	1
20	4.37	3.171	11.178	1

HEP-2				
MBHA	**pIC_{50}**	**E3s**	**RDF085v**	**σ_p**
1	5.46	0.164	0	0
2	5.39	0.145	0	0
3*	5.63	0.146	0.158	0
5	5.23	0.091	0.002	0.78
6	5.22	0.106	0.265	0.78
7	5.28	0.107	0.1	0.23
8	5.67	0.104	0.559	0.23
9	5.4	0.138	0.764	0.23
10	4.31	0.283	1.602	0
11	4.41	0.228	1.728	0
12	4.48	0.212	2.572	0
14	4.67	0.15	1.528	0.78
15	4.51	0.151	2.473	0.78
16*	5.17	0.186	1.388	0.23
18	4.72	0.148	5.455	0.23
20	4.72	0.13	5.771	0.23
21	4.37	0.154	7.051	0.23

HL-60				
MBHA	**pIC_{50}**	**R2u**	**R7p**	**G3p**	**RDF095p**
1	5.44	1.34	0.085	0.195	0
2	5.75	1.473	0.136	0.219	0
3*	5.73	1.462	0.274	0.188	0.001
5	5.53	1.43	0.203	0.212	0
6	7.85	1.424	0.317	0.217	0.144
7	5.88	1.26	0.166	0.195	0
8*	5.84	1.408	0.228	0.198	0
9	7.88	1.413	0.377	0.188	0.02
10	4.56	1.525	0.183	0.172	0.068
11	4.76	1.663	0.221	0.203	0.071
12	4.79	1.648	0.322	0.163	0.139
14	5.2	1.616	0.267	0.197	0.395
15	5.26	1.611	0.346	0.195	0.574
16	5.32	1.449	0.254	0.172	0.899
17	5.37	1.603	0.304	0.186	1.378
18	4.74	1.632	0.272	0.206	5.461
19	5.26	1.583	0.332	0.182	6.548
20*	5.26	1.615	0.342	0.186	5.51
21	4.84	1.576	0.413	0.176	8.089

*Test set

Validation parameters are presented in the Table 4, attesting good QSAR models, with robustness and predictability.

$$MCF7 = + 0.2987(\mathbf{L2p}) - 0.0601(\mathbf{RDF085u}) - 0.5050(\mathbf{N\text{-}R}) + 4.5639 \tag{1}$$

$$HEP\text{-}2 = - 7.7568\,(\mathbf{E3s}) - 0.1127\,(\mathbf{RDF085v}) - 0.7150(\mathbf{\sigma p}) + 6.5590 \tag{2}$$

$$HL\text{-}60 = - 5.8846(\mathbf{R2u}) + 9.5500(\mathbf{R7p}) + 25.4131(\mathbf{G3p}) - 0.1369(\mathbf{RDF095p}) + 7.2700 \tag{3}$$

Table 4. Validation parameters of QSAR models

Model	R^2	R^2_{adj}	R_{cal}	Q^2	Q^2_{ext}	s	F
MCF-7	0.87	0.83	0.93	0.75	0.73	0.16	22.76
HEP-4	0.91	0.88	0.95	0.84	0.77	0.17	34.00
HL-60	0.83	0.77	0.91	0.60	0.68	0.46	13.69

In the QSAR analysis, it is important interpretation of the physical sense of the molecular descriptors, which must be related to biological activity profile, providing discussions about the structure-activity relationship. The analysis stills the designing and prediction of new potentially more active compounds

Considering a general analysis for the three models, we can observe that highest values of **L2p**, **R7p** and **G3p** descriptors tends to increase biological profile, and are related to molecules with allyl moiety at nitrogen of oxindole scaffold.[23] Descriptor named N-R (Isatin nitrogen with substituent) have negative regression coefficient, but this descriptor must be related to substituted methyl and not allyl as responsible to decrease the activity. In fact, **2**, **5**, **8**, **11**, **14**, **17** have CH_3 and four of them have $pIC_{50} < 5.0$ (less active), while **3**, **6**, **9**, **12**, **15** have allyl moiety and just **12** have $pIC_{50} < 5.0$. **RDF085u**, **RDF085v**, **RDF095p**, **E3s**, **R2u** are descriptors related to the probability distribution of finding an atom in a spherical volume, as well the volume and shape of molecules.[23] Their regression coefficients are negative, thus, most compact molecules, as nitrile derivatives, tend to better cytotoxic activities, instead of methyl ester or larger amide groups (**10-21**). σ_p is the Hammett constant on para position of aromatic ring, related to isatin nitrogen. Higher values (electrons withdraw groups) decrease the activity in HEP-2 cell line, according to the negative regression coefficient.

The ADME profiles of the analyzed compounds are shown in the Table 5. Observing the Total Polar Surface Area (TPSA) and Consensus LogP parameters, the most highlighted compounds in activity and selectivity, **6** and **9** (Figure 3), presented different profiles, where the last have minor value of polar surface and better lipophilic balance (between 2-5), denoting a better absorption in organism. However, the BBB penetration can represent a problem, if the compound affects the Central Nervous System with adverse effects, by which the compound **6** was predicted with no susceptibility for BBB penetration, and **9** have a check "yes" (Table 5). In addition, the highest superficial

polarity of the **6** can decreases its ability to act as an inhibitor of the metabolism enzymes, as reflected in the CYP complex parameter, having fewer possibilities than **9**. In a summarization, the Abbot Bioavailability Score seeks to predict the probability of a compound to have at least 10% oral bioavailability in rat or measurable Caco-2 permeability.[20] This semi-quantitative rule-based score relying on total charge, TPSA, and violation to the Lipinski filter, defines four classes of compounds with probabilities of 11%, 17%, 56% or 85%.[20] Overall, our evaluated the compounds have a equally moderate Drug-likeness profile, greater than 50%, checking all the Drug-like rules with "Yes" (Table 5).
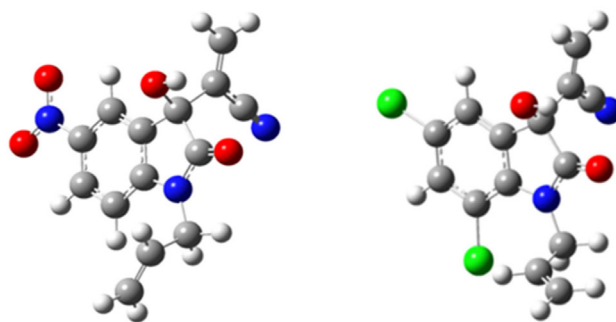

Figure 3. 3D visualization of the highlighted compounds **6** (left) and **9** (right), which presented moderate to highest activities (four cell lines) and the highest SI (HL-60)

Table 5. Calculated ADME profile by the SwissADME platform, for the compounds with determined SI

| Physicochemical Properties	Morita-Baylis-Hillman adducts						
	2	3	5	6	7	8	9
Formula	$C_{13}H_{12}N_2O$	$C_{15}H_{14}N_2O$	$C_{13}H_{11}N_3O_3$	$C_{15}H_{13}N_3O_3$	$C_{12}H_8Cl_2N_2O$	$C_{13}H_{10}Cl_2N_2O$	$C_{15}H_{12}Cl_2N_2O$
Molecular weight	212.25 g/mol	238.28 g/mol	257.24 g/mol	283.28 g/mol	267.11 g/mol	281.14 g/mol	307.17 g/mol
Num. heavy atom	16	18	19	21	17	18	20
Num. Arom. heavy atom	6	6	6	6	6	6	6
Fraction Csp³	0.15	0.13	0.15	0.13	0.08	0.15	0.13
Num. Rotatable bonds	1	3	2	4	1	1	3
Num. H-bond acceptors	2	2	4	4	2	2	2
Num. H-bond donors	1	1	1	1	2	1	1
Molar refractivity	65.51	74.65	74.33	83.47	70.63	75.53	84.67
TPSA*	47.26	47.26	93.08	93.08	56.05	47.26	47.26
Log $P_{o/w}$ (ILOGP)	2.05	2.53	1.80	2.07	2.28	2.52	2.70
Log $P_{o/w}$ (XLOGP3)	2.13	2.77	1.96	2.60	3.24	3.38	4.03
Log $P_{o/w}$ (WLOGP)	1.43	1.98	1.34	1.89	2.52	2.74	3.29
Log $P_{o/w}$ (MLOGP)	1.15	1.58	0.13	0.57	1.94	2.20	2.61
Log $P_{o/w}$ (SILICOS-IT)	1.97	2.72	- 0.17	0.59	3.33	3.26	4.02
Consensus Log $P_{o/w}$	1.74	2.32	1.01	1.54	2.66	2.82	3.33
Pharmacokinetics	**2**	**3**	**5**	**6**	**7**	**8**	**9**
GI absorption	High	High	High	High	High	High	High
BBB permeant	Yes	Yes	No	No	Yes	Yes	Yes
P-gp substrate	No	No	No	No	No	No	No
CYP1A2 inhibitor	Yes	Yes	No	Yes	Yes	Yes	Yes
CYP2C19 inhibitor	No	Yes	No	No	Yes	Yes	Yes
CYP2C9 inhibitor	No	Yes	No	Yes	Yes	Yes	Yes
CYP2D6 inhibitor	No	No	No	No	No	No	No
CYP3A4 inhibitor	No	No	No	No	Yes	Yes	Yes
Log Kp (skin permeation)	- 6.08 cm/s	- 5.79 cm/s	- 6.48 cm/s	- 6.18 cm/s	- 5.63 cm/s	- 5.62 cm/s	- 5.31 cm/s
Drug-likeness	**2**	**3**	**5**	**6**	**7**	**8**	**9**
Lipinski	Yes	Yes	Yes	Yes	Yes	Yes	Yes
Ghose	Yes	Yes	Yes	Yes	Yes	Yes	Yes
Veber	Yes	Yes	Yes	Yes	Yes	Yes	Yes
Egan	Yes	Yes	Yes	Yes	Yes	Yes	Yes
Muegge	Yes	Yes	Yes	Yes	Yes	Yes	Yes
Bioavailability Score	0.55	0.55	0.55	0.55	0.55	0.55	0.55

*TPSA unit in Å²
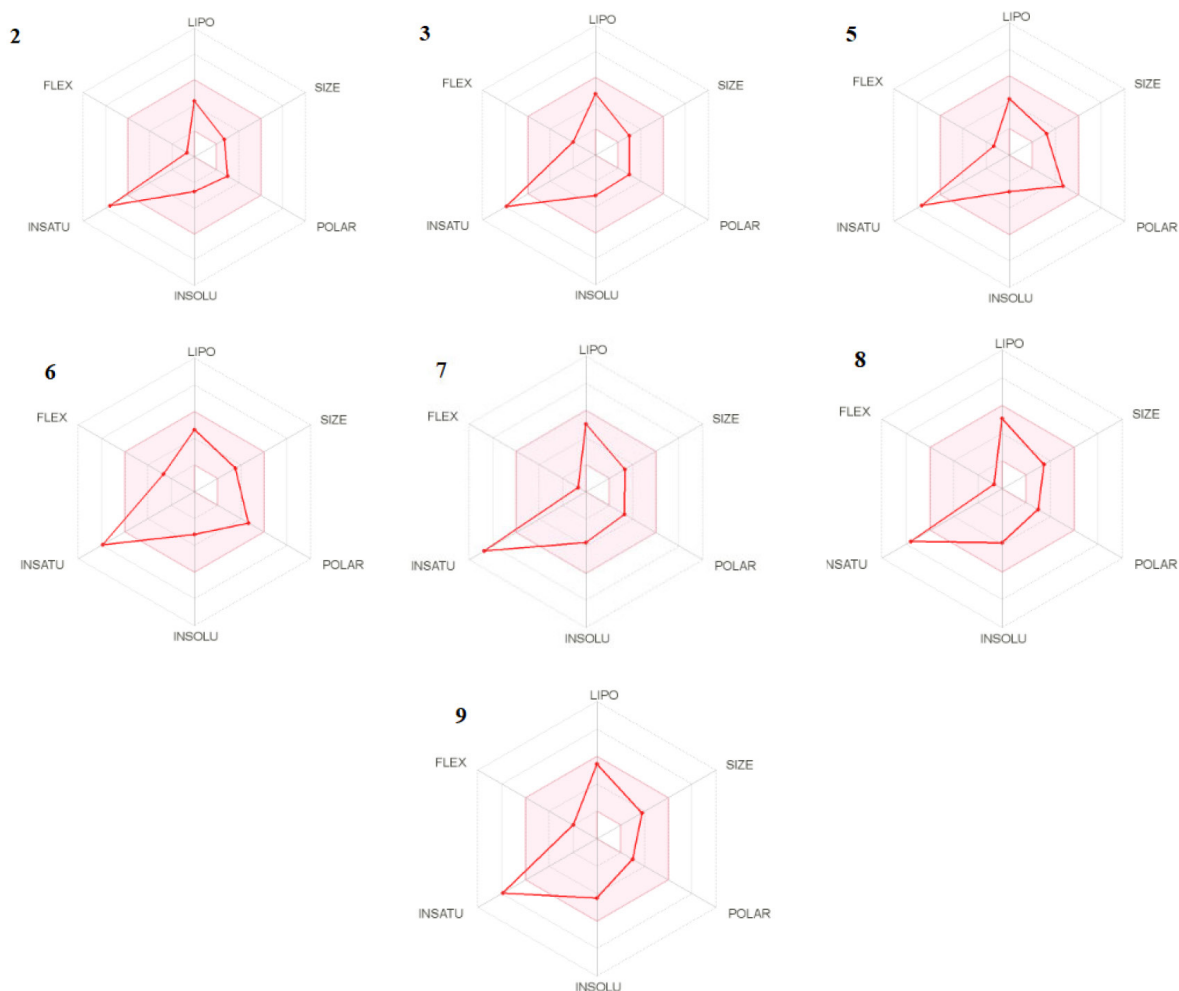
Figure 4. Bioavailability Radar graphs by SwissADME platform for analyzed compounds

Finally, the Figure 4 shows the Bioavailability Radar, which represents a rapid and general visualization of the drug-likeness.[20] Six physicochemical properties are taken into account: lipophilicity, size, polarity, solubility, flexibility and saturation. A physicochemical range on each axis is defined by some descriptors and depicted as a pink area,[24,25] in which the radar plot of the molecule has to fall entirely to be considered drug-like.[24] We can observe that all the compounds are in pink area, except by the saturation parameter. This term represents a fraction of carbons in the sp[3] hybridization (Fsp[3]) higher than 0.25,[25] which can represent a better 3D distribution for molecular recognition and better solubility.[25] However, we must remember that the isatin ring has an expressive degree of unsaturation, leading to decreasing in Fsp[3] factor. This fact reveals a guideline for future synthesis, expanding the number of atoms in the 6-membered ring with saturated alkyl moieties or/and N-isatin substituent groups, in order to better adjust this parameter.

Thus, considering quantitative and qualitative analysis described above, supported by *in silico* approaches, Morita-Baylis-Hillman adducts from isatin derivatives with nitrile moiety and longer alkyl substituents on isatin nitrogen (as allyl group) tend to be more cytotoxic on cancer cell lines. The QSAR models can be used to predict the tendency of activity for new analogs and SwissADMET results revealed other important aspects to take in account in future studies.

4. Conclusions

In this paper, we presented the antiproliferative activity of twenty one Morita-Baylis-Hillman from isatin derivatives. Except by of MCF-7 cell line, we reported new compounds with higher selectivity index than Doxorubicin (standard drug), especially **6** and **9,** in HL-60 cell line. This makes the Morita-Baylis-Hillman adducts from isatin derivatives a promissory class in the search of new anticancer compounds, for posterior synthesis and/or in vivo screenings. Qualitative analysis, QSAR modellings and SwissADME parameters allowed the rationalization of the experimental data, reinforcing the importance of the nitrile and allyl moieties in a future synthetic planning, altering only the substituents on the aromatic ring and possibly expanding the allyl substituent, aiming best activities, selectivity and ADME profile.

Acknowledgements

References

1. Ferlay, J.; Colombet, M.; Soerjomataram, I.; Mathers, C.; Parkin, D. M.; Piñeros, M.; Znaor, A.; Bray, F.; Estimating the global cancer incidence and mortality in 2018: GLOBOCAN sources and methods. *International Journal of Cancer* **2019**, *144*, 1941. [Crossref]

2. Nurgali, K.; Thomas, J. R.; Abalo, R.; Editorial: Adverse Effects of Cancer Chemotherapy: Anything New to Improve Tolerance and Reduce Sequelae? *Front Pharmacol* **2018**, *9*, 245. [Crossref]

3. Silva, R. B.; Torres, J. C.; Garden, S. J.; Violante, F. A.; Rezende, M. J. C.; Silva, B. V.; Pinto, A. C.; From the isolation to the synthesis of convolutamydine A. *Química Nova* **2008**, *31*, 924. [Crossref]

4. Santos, M. S.; Coelho, F.; Lima-Junior, C. G.; Vasconcellos, M. L. A. A.; The Morita-Baylis-Hillman Reaction: Advances and Contributions from Brazilian Chemistry. *Current Organic Synthesis* **2015**, *12*, 830. [Crossref]

5. Junior, C. G. L.; Silva, F. P. L.; Oliveira, R. G.; Subrinho, F. L.; Andrade, N. G.; Vasconcellos, M. L. A. A.; Microwave irradiation or low temperature improved synthesis of antiparasitic Morita-Baylis-Hillman adducts. *Journal of the Brazilian Chemical Society* **2011**, *22*, 2220. [Crossref]

6. Brito, V. B. M.; Santos, G. F.; Silva, T. D. S.; Souza, J. L. C.; Militão, G. C. G.; Martins, F. T.; Silva, F. P. L.; Oliveira, B. G.; Araújo, E. C. C.; Vasconcellos, M. L. A. A.; Lima-Júnior, C. G.; Alencar-Filho, E. B.; Synthesis, anti-proliferative activity, theoretical and 1H NMR experimental studies of Morita–Baylis–Hillman adducts from isatin derivatives. *Molecular Diversity* **2020**, *24*, 265. [Crossref]

7. Liao, C.; Sitzmann, M.; Pugliese, A.; Nicklaus, M. C.; Software and resources for computational medicinal chemistry. *Future Medicinal Chemistry* **2011**, *3*, 1057. [Crossref]

8. Cherkasov, A.; Muratov, E. N.; Fourches, D.; Varnek, A.; Baskin, I. I.; Cronin, M.; Dearden, J.; Gramatica, P.; Martin, Y. C.; Todeschini, R.; Consonni, V.; Kuz'min, V. E.; Cramer, R.; Benigni, R.; Yang, C.; Rathman, J.; Terfloth, L.; Gasteiger, J.; Richard, A.; Tropsha, A.; QSAR modeling: where have you been? Where are you going to? *Journal of Medicinal Chemistry* **2014**, 57, 4977. [Crossref] [PubMed]

9. Alencar-Filho, E. B.; Moraes, I. A.; Weber, K. C.; Rocha, G. B.; Vasconcellos, M. L. A. A.; DFT/PCM, QTAIM, 1H NMR conformational studies and QSAR modeling of thirty-two anti-Leishmania amazonensis Morita–Baylis–Hillman Adducts. *Journal of Molecular Structure* **2012**, *1022*, 72. [Crossref]

10. Stewart, J. J. P.; Optimization of parameters for semiempirical methods. V. Modification of NDDO approximations and application to 70 elements. *Journal of Molecular Modeling* **2007**, *13*, 1173. [Crossref]

11. Becke, A. D.; Density functional thermochemistry. III. The role of exact exchange. *The Journal of Chemical Physics* **1993**, *98*, 5648. [Crossref]

12. Lee, C.; Yang, W.; Parr, R. G.; Development of the Colle-Salvetti correlation-energy formula into a functional of the electron density. *Physical Review B* **1988**, *37*, 785. [Crossref]

13. Vosko, S. H.; Wilk, L.; Nusair, M.; Accurate spin-dependent electron liquid correlation energies for local spin density calculations: a critical analysis. *Canadian Journal of Physics* **1980**, *58*, 1200. [Crossref]

14. Gaussian 09, Revision A.01, Frisch, M. J.; Trucks, G. W.; Schlegel, H. B.; Scuseria, G. E.; Robb, M. A.; Cheeseman, J. R.; Scalmani, G.; Barone, V.; Mennucci, B.; Petersson, G. A.; Nakatsuji, H.; Caricato, M.; Li, X.; Hratchian, H. P.; Izmaylov, A. F.; Bloino, J.; Zheng, G.; Sonnenberg, J. L.; Hada, M.; Ehara, M.; Toyota, K.; Fukuda, R.; Hasegawa, J.; Ishida, M.; Nakajima, T.; Honda, Y.; Kitao, O.; Nakai, H.; Vreven, J.; Montgomery, J. A.; Jr-Peralta, J. E.; Ogliaro, F.; Bearpark, M.; Heyd, J. J.; Brothers, E.; Kudin, K. N.; Staroverov, V. N.; Kobayashi, R.; Normand, J.; Raghavachari, K.; Rendell, A.; Burant, J. C.; Iyengar, S. S.; Tomasi, J.; Cossi, M.; Rega, N.; Millam, J. M.; Klene, M.; Knox, J. E.; Cross, J. B.; Bakken, V.; Adamo, C.; Jaramillo, J.; Gomperts, R.; Stratmann, R.; E-Yazyev, O.; Austin, A. J.; Cammi, R.; Pomelli, C.; Ochterski, J. W.; Martin, R. L.; Morokuma, K.; Zakrzewski, V. G.; Voth, G. A.; Salvador, P.; Dannenberg, J. J.; Dapprich, S.; Daniels, A. D.; Farkas, O.; Foresman, J. B.; Ortiz, J. V.; Cioslowski, J.; Fox, D. J.; Gaussian, Inc.; Wallingford, C. T. available in: < https://gaussian.com/g09citation/>. Access in: 31 January 2021.

15. Tetko, I. V.; Gasteiger, J.; Todeschini, R.; Mauri, A.; Livingstone, D.; Ertl, P.; Palyulin, V. A.; Radchenko, E. V.; Zefirov, N. S.; Makarenko, A. S.; Tanchuk, V. Y.; Prokopenko, V. V. J.; Virtual computational chemistry laboratory - design and description. *Journal of Computer-Aided Molecular* Design **2005**, *19*, 453. [Crossref]

16. Teófilo, R. F.; Martins, J. P. A.; Ferreira, M. M. C.; Sorting variables by using informative vectors as a strategy for feature selection in multivariate regression. *Journal of Chemometrics* **2009**, *23*, 32. [Crossref]

17. Martins, J. P. A.; Ferreira, M. M. C.; QSAR modeling: a new open source computational package to generate and validate QSAR models. *Química Nova* **2013**, 36, 554. [Crossref]

18. De Oliveira, D. B.; Gaudio, A. C.; BuildQSAR: A New Computer Program for QSAR Analysis. *Quantitative Structure-Activity Relationships* **2000**, *19*, 599. [Crossref]

19. Kiralj, R.; Ferreira, M. M. C.; Basic validation procedures for regression models in QSAR and QSPR studies: theory and application. *Journal of the Brazilian Chemical Society* **2009**, *20*, 770. [Crossref]

20. Daina, A.; Michielin, O.; Zoete, V.; SwissADME: a free web tool to evaluate pharmacokinetics, drug-likeness and medicinal chemistry friendliness of small molecules. *Scientific Reports* **2017**, *7*, 42717. [Crossref] [PubMed]

21. Fleming, F. F.; Yao, L.; Ravikumar, P. C.; Funk, L.; Shook, B. C.; Nitrile-Containing Pharmaceuticals: Efficacious Roles of the Nitrile Pharmacophore. *Journal of Medicinal Chemistry* **2010**, *53*, 7902. [Crossref] [PubMed]

22. Fortes, M. P.; da Silva, P. B. N.; da Silva, T. G.; Kaufman, T. S.; Militão, G. C. G.; Silveira, C. C.; Synthesis and preliminary evaluation of 3-thiocyanato-1H-indoles as potential anticancer agents. *European Journal of Medicinal Chemistry* **2016**, *118*, 21. [Crossref]

23. Todeschini, R.; Consonni, V.; *Molecular descriptors for chemoinformatics*, Volume I: Alphabetical Listing, 2nd ed., Wiley-VCH: New York, 2009**.** [Crossref]

24. Ritchie, T. J.; Ertl, P.; Lewis, R.; The graphical representation of ADME-related molecule properties for medicinal chemists. *Drug Discovery Today* **2011**, *16*, 65. [Crossref] [PubMed]

25. Lovering, F.; Bikker, J.; Humblet, C.; Escape from Flatland: Increasing Saturation as an Approach to Improving Clinical Success. *Journal of Medicinal Chemistry* **2009**, *52*, 6752. [Crossref]